Taylor & Francis
Taylor & Francis Group

Canadian Journal of Remote Sensing
Journal canadien de télédétection

ISSN: 0703-8992 (Print) 1712-7971 (Online) Journal homepage: http://www.tandfonline.com/loi/ujrs20

Biparabolic NDVI-T_s Space and Soil Moisture Remote Sensing in an Arid and Semi arid Area

Ying Liu, Lixin Wu & Hui Yue

To cite this article: Ying Liu, Lixin Wu & Hui Yue (2015) Biparabolic NDVI-T_s Space and Soil Moisture Remote Sensing in an Arid and Semi arid Area, Canadian Journal of Remote Sensing, 41:3, 159-169, DOI: 10.1080/07038992.2015.1065705

To link to this article: http://dx.doi.org/10.1080/07038992.2015.1065705

Canadian Journal of Remote Sensing, 41:159–169, 2015

ISSN: 0703-8992 print / 1712-7971 online
DOI: 10.1080/07038992.2015.1065705

Taylor & Francis
Taylor & Francis Group

Biparabolic NDVI-T_s Space and Soil Moisture Remote Sensing in an Arid and Semi arid Area

Ying Liu[1,*], Lixin Wu[2,3], and Hui Yue[1]

[1]*Xi'an University of Science and Technology, College of Geomatics, Yanta Road, Xi'an, 710054, China*
[2]*China University of Mining and Technology, School of Environment Science and Spatial Informatics, Daxue Road, Xuzhou, 221116, China*
[3]*Northeastern University, Institute for Geoinformatics & Digital Mine Research, Heping District, Shenyang, 110819, China*

Abstract. Normalized difference vegetation index (NDVI) and land surface temperature (T_s) data from the multitemporal Moderate Resolution Imaging Spectroradiometer (MODIS) were used to analyze the NDVI-T_s space. Unlike the traditional triangular or trapezoidal NDVI-T_s space, the NDVI-T_s space in this study was biparabolic when NDVI values below 0.15 were included, describing areas that are vegetated but have low biomass due to arid conditions. Moreover, the NDVI-T_s biparabolic space is slightly better than the NDVI-T_s triangular space at discerning soil moisture (validation at a 10-cm depth). Linear relationships exist between $TVDI_C$ obtained from the NDVI-T_s biparabolic space and relative soil moisture with $R^2 > 0.28$, while correlation coefficient between $TVDI_T$ obtained from the triangular NDVI-T_s space and relative soil moisture is $R^2 > 0.08$. The soil moisture situations in Henan Province from February 26, 2011 to May 16, 2011 and in the Shendong mining area on October 8, 2010 were evaluated based on the temperature vegetation dryness index (TVDI) obtained from the NDVI-T_s biparabolic space. Moreover, the general spatiotemporal features of soil moisture conditions in Henan Province and the Shendong mining area were revealed.

Résumé. Des données de l'indice de végétation par différence normalisé (NDVI) et de la température de la surface terrestre (T_s) du spectroradiomètre imageur à résolution moyenne «Moderate Resolution Imaging Spectroradiometer» (MODIS) ont été utilisées pour analyser l'espace NDVI-T_s. Contrairement à l'espace traditionnel NDVI-T_s qui est triangulaire ou trapézoïdal, l'espace NDVI-T_s dans cette étude était biparabolique lorsque les valeurs de NDVI inférieures à 0,15 ont été incluses, décrivant les régions qui ont un couvert végétal, mais qui ont une faible biomasse en raison des conditions arides. En outre, l'espace biparabolique NDVI-T_s est légèrement mieux que l'espace triangulaire NDVI-T_s pour discerner l'humidité du sol (validation à une profondeur de 10 cm). Des relations linéaires existent entre le $TVDI_C$ obtenu à partir du NDVI-T_s biparabolique et l'humidité du sol relative avec $R^2 > 0{,}28$, tandis que le coefficient de corrélation entre le $TVDI_T$ obtenu à partir de l'espace NDVI-T_s triangulaire et l'humidité du sol relative est $R^2 > 0{,}08$. L'humidité du sol dans la province du Henan du 26 février 2011 au 16 mai 2011 et dans la région d'exploitation minière Shendong le 8 octobre 2010 a été évaluée sur la base de l'indice de température-sécheresse de la végétation (TVDI) obtenu à partir de l'espace biparabolique NDVI-T_s. En outre, les caractéristiques générales spatio-temporelles de conditions d'humidité du sol dans la province du Henan et la zone minière Shendong ont été révélées.

INTRODUCTION

Soil moisture is one of the most important environmental variables. It not only integrates land surface hydrology, but also plays a critical role in evaluating hydrological, meteorological, and agricultural processes (Sun et al. 2012). Variations in soil moisture produce essential changes in surface energy balance, regional runoff, and vegetation productivity (Han et al. 2010). For this reason, spatiotemporal distributions and changes in soil moisture should be monitored. Monitoring soil moisture using remotely sensed satellite data has become a popular research focus worldwide (Sun et al. 2012; Sela et al. 2012; Skierucha et al. 2014; Muñoz-Sabater 2015).

Remote sensing technology can provide land surface parameters such as normalized difference vegetation index (NDVI), land surface temperature (T_s), and albedo (Tang et al. 2010). The combination of NDVI and T_s, which is widely used to study land surface processes, can provide significant information on land surface vegetation and soil moisture conditions. Numerous studies have explored the relationship between NDVI and T_s and can be grouped into 4 broad categories (Carlson 2007; Han et al. 2010; Karnieli et al. 2010).

(i) A strong negative relationship between NDVI and T_s has been widely observed ($R^2 = 0.73$–0.91; Goward et al. 1985; Hope et al. 1986; Nemani et al. 1989). The slope

Received 30 October 2014. Accepted 11 June 2015.
*Corresponding author e-mail: liuying712100@163.com

of the T_s/NDVI curve can provide insights into stomatal resistance, evapotranspiration, and land surface soil water content. Nemani et al. (1993) found that the T_s/NDVI combination typically shows a strong negative relationship in different land use types and that the slope of T_s/NDVI is strongly correlated with the crop-moisture index and, therefore, can discern soil moisture conditions. However, a positive relationship between NDVI and T_s has also been observed. Lambin and Ehrlich (1996) stated that changes in NDVI are positively correlated over time with changes in T_s when energy is the main factor limiting vegetation. However, changes in NDVI can be expected to be negatively correlated over time to changes in T_s when water is the main factor limiting vegetation, such as in dry regions.

(ii) Price (1990) and Carlson et al. (1994) indicated that a scatterplot of T_s and NDVI often results in a triangular shape when a full range of fractional vegetation cover and soil water content is represented in the data. Triangular NDVI-T_s spaces are widely used to estimate surface soil moisture conditions, surface evapotranspiration conditions, drought conditions, and land cover and land use changes (Chen et al. 2011; Sun et al. 2011; Gao et al. 2011; Juliena et al. 2011; Rahimzadeh-Bajgiran et al. 2012; Sona et al. 2012; Li et al. 2012; Girolimetto and Venturini 2013).

(iii) Goward and Hope (1989) and Moran et al. (1994) claimed that a scatterplot of T_s and NDVI often demonstrates a trapezoidal shape. Moran et al. (1994) extended the crop water stress index to a water deficit index (WDI) using a trapezoidal NDVI-T_s space. The WDI provides accurate estimates of field evapotranspiration rates and relative field water deficit for both full-cover and partially vegetated sites.

(iv) Sandholt et al. (2002) developed a temperature vegetation dryness index (TVDI) using a triangular NDVI-T_s space to estimate temporal and spatial soil moisture patterns. The index, which is related only to remotely sensed data, is conceptually and computationally straightforward. Wang et al. (2001) developed a vegetation temperature condition index (VTCI) based on a triangular NDVI-T_s space. VTCI analysis was carried out for drought monitoring in the Guanzhong Plain area of the Loess Plateau in northwestern China. The VTCI can monitor regional drought occurrence and capture spatial variations in drought. The TVDI and the VTCI are widely used to monitor land surface soil water content and drought conditions.

Both TVDI and VTCI are based on linear dry and wet edges, which can be obtained from a scatter plot of T_s and NDVI in the area. However, in studies by Price (1990) and Carlson et al. (1994), it was found that the dry edge exhibited a parabolic shape in a scatter plot of T_s and NDVI. Carlson et al. (1994) also pointed out that the dry edge was highly nonlinear at both low and high NDVI values. Gillies and Carlson (1995) reproduced a 4th-order polynomial to describe the borders of the dry edge in the NDVI-T_s space. These studies showed that the dry edge is not always linear in a triangular NDVI-T_s space.

Previous studies have shown that the land surface is bare and not covered by vegetation when NDVI < 0.15, and therefore this part of the relationship was removed when finding a linear fit of the dry edge (Lu et al. 2007). NDVI values below 0.15 are found in areas with low biomass in arid regions. In this study, we examined the NDVI-T_s space in an experimental region in the Shendong mining district of China and developed a biparabolic relationship. This method was compared with a triangular NDVI-T_s space at a verification site in China. Finally, TVDI, as obtained from the biparabolic NDVI-T_s space, was used to reveal the spatiotemporal features of soil moisture in the Shendong mining area and Henan Province in comparison with field-measured soil moisture.

STUDY AREA AND DATA

Shendong Mining Area

The Shendong mining area (Figure 1) is located in the southeastern portion of the Ordos Plateau, on the northern edge of the Loess Plateau in northern Shaanxi and the southeastern edge of the Mu Us Desert, and is centred at (110° 18′ 30″ E, 39° 11′ 30″ N). This mining area is one of the major coal production centers in China and belongs to an arid and semiarid desert mining area. The ecological environment of the Shendong mining area is fragile, and the climate is characterized by low precipitation, uneven seasonal distribution, strong evaporation, and scarcity of surface water resources. Soil moisture is the dominant factor in vegetation growth and recovery in this area.

Henan Province

Henan Province, located in an arid and semiarid area, is the main producing region for grain crops in China. Farmland accounts for approximately 69.18% of the land area of the province (Figure 2). Spring in Henan Province is often very dry, which is detrimental to crop growth and threatens the summer harvest. Therefore, remote sensing monitoring of soil moisture for winter wheat in Henan Province is essential.

Data

NDVI and T_s are the main parameters used for soil-moisture monitoring when using MODIS data. The 2 MODIS data products used in the Shendong mining area were the reflectivity dataset (MYD09GA) with 500-m resolution and the land surface temperature (MYD11A1) dataset with 1-km resolution, both collected on October 8, 2010.[1]

[1]Data were downloaded from http://reverb.echo.NASA.gov/reverb/.

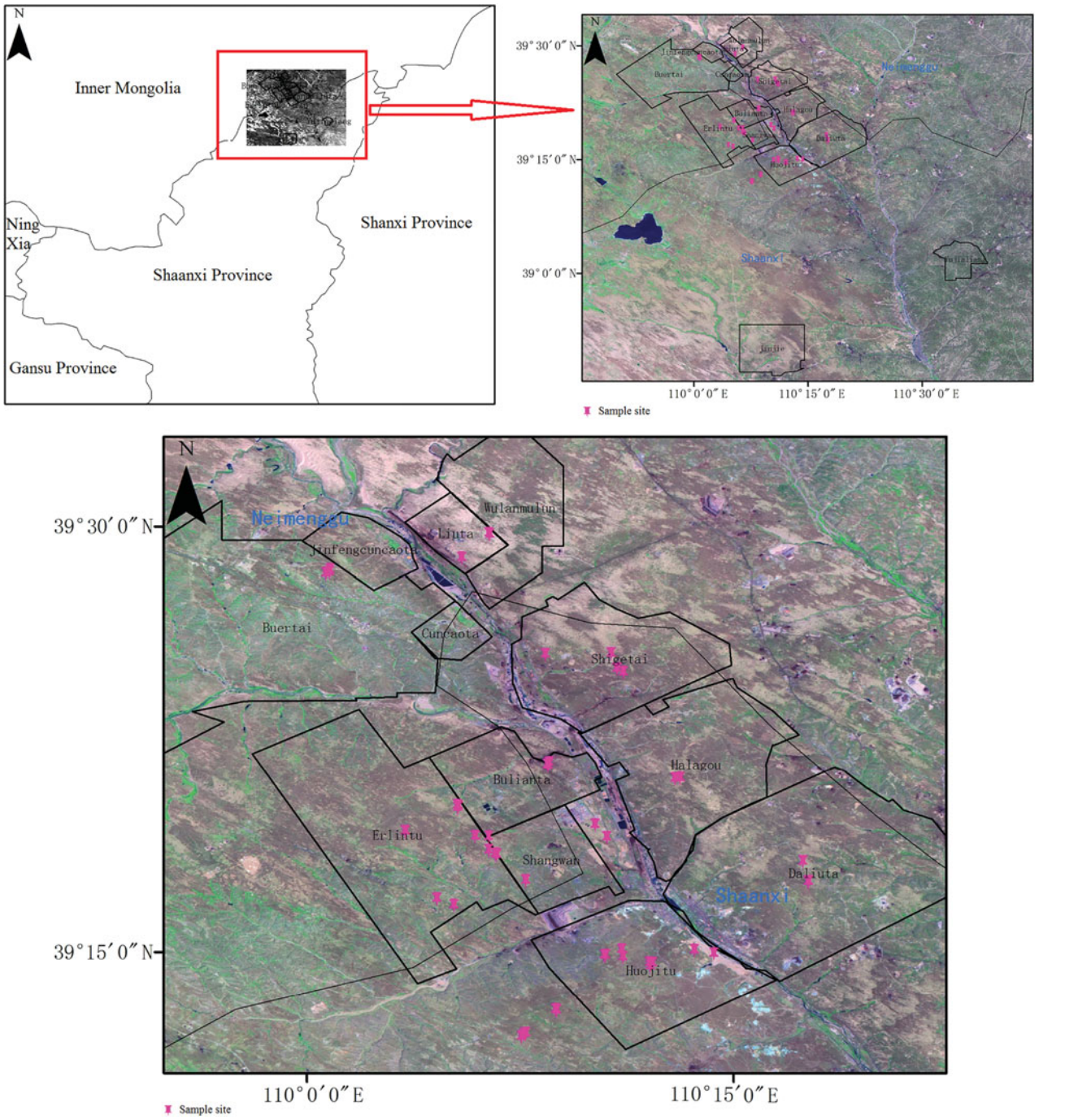

FIG. 1. Map of the experimental area.

The NDVI with 1-km resolution can be obtained from the 16-day composite ground vegetation index (MYD13A2), and T_s with 1-km resolution can be obtained from the 8-day composite land-surface temperature (MYD11A2) from February 26, 2011 to May 16, 2011 in Henan Province. The 2 temporal-phase, 8-day composite T_s datasets were processed to match a single temporal-phase, 16-day composite NDVI image.

Data processing was carried out as follows: (*i*) infrared and near-infrared reflectance data were obtained from MYD09GA to calculate the NDVI of the study area, and (*ii*) T_s was obtained from MYD11A1 for the study area. The T_s data were resampled to 500-m resolution to match the 500-m resolution NDVI image.

Data on relative soil moisture to compare with TVDI were obtained in 2 ways: field sample, and collection from weather

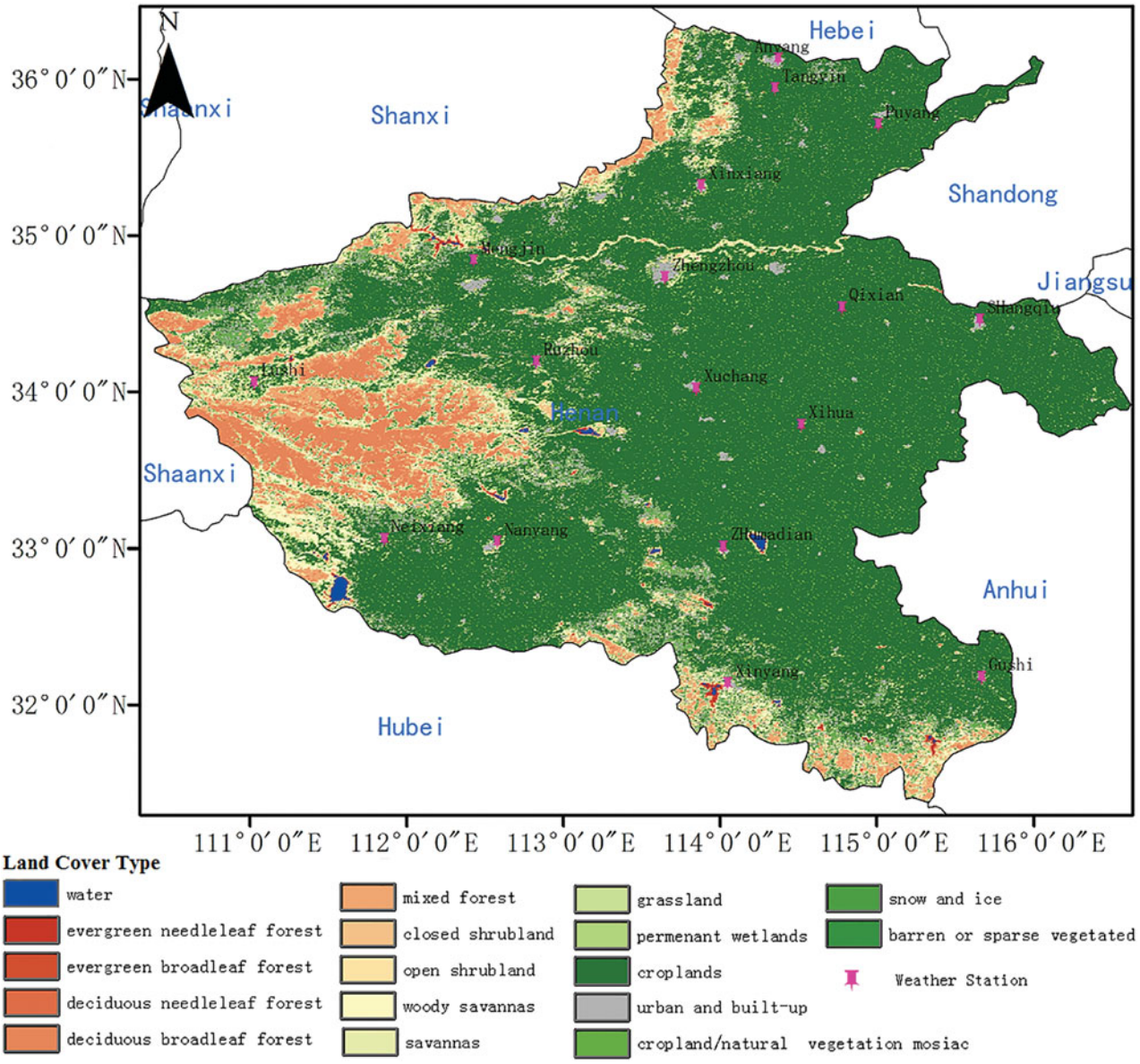

FIG. 2. Land use types in Henan Province.

stations. Soil samples from the Shendong site were taken back to the laboratory, and a traditional weighing method was used to obtain relative soil moisture (Figure 1). The number of field sample points was 47. Relative soil moisture was derived from 17 weather stations at the Henan site (Figure 2), yielding 17 sample points.

METHODS

Experiments

The Shendong mining area was taken as the experimental site. Figure 3a shows a scatter plot of the dry and wet edges in the NDVI-T_s space for the experimental area. The figure shows that the NDVI-T_s space is biparabolic, with the dry-edge position relationship having a high correlation coefficient $R^2 > 0.85$ and the wet-edge position relationship having a correlation coefficient $R^2 > 0.7$.

A Description of the Triangular Method

Sandholt et al. (2002) developed a simplified land surface dryness index based on the triangular NDVI-T_s space, i.e., the TVDI (Figure 4), which can be expressed as follows:

$$\mathrm{TVDI} = \frac{T_s - T_{s\min}}{T_{s\max} - T_{s\min}}, \qquad [1]$$

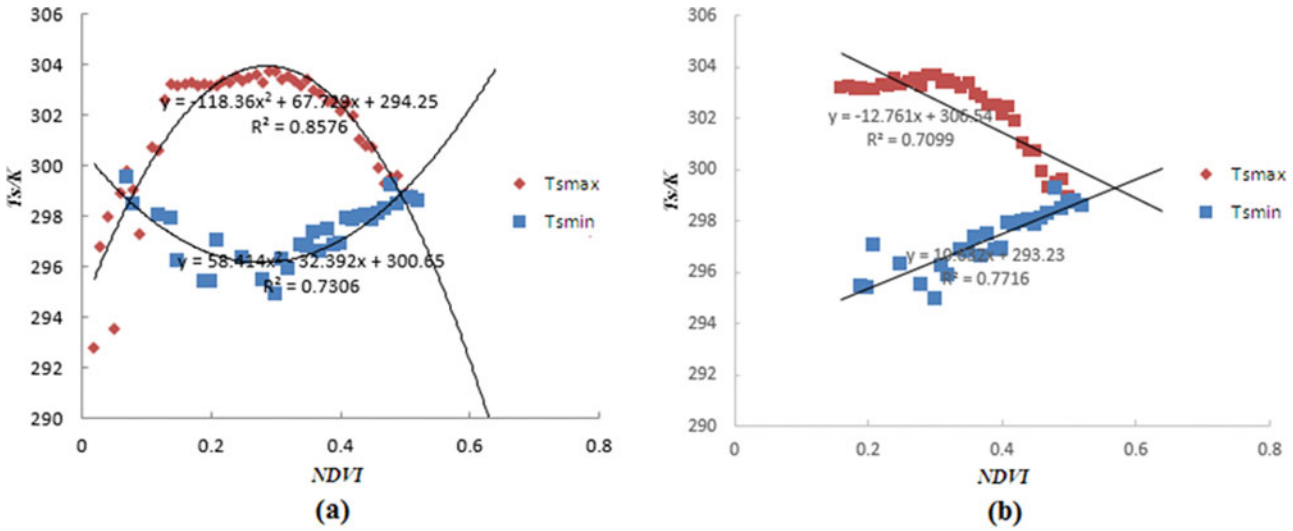

FIG. 3. Scatter plot of dry and wet edges in the NDVI-T_s space in the Shendong mining area: (a) biparabolic NDVI-T_s space; (b) triangular NDVI-T_s space.

where

$$T_{s\,max} = a_1 + b_1 \times \text{NDVI}$$
$$T_{s\,min} = a_2 + b_2 \times \text{NDVI}, \quad [2]$$

where T_s is the observed surface temperature at the given pixel; $T_{s\,min}$ is the minimum surface temperature in the triangle, defining the wet edge; and $T_{s\,max}$ is the maximum surface temperature observation for a given NDVI, defining the dry edge; a_2 and b_2 define the dry edge as a linear fit to the data; and a_1 and b_2 define the wet edge, which is the minimum surface temperature in the triangle.

The value of the TVDI ranges from 0 to 1. A larger TVDI means that T_s is closer to the dry edge and that the dryness condition is more serious. By contrast, a smaller TVDI means that T_s is closer to the wet edge and the soil condition is moister.

Biparabolic NDVI-T_s Space Method

The principle of the triangular or trapezoidal NDVI-T_s spaces is that the NDVI is expected to be negatively correlated with changes in T_s. Values of NDVI below 0.15 were often eliminated in the linear fitting of the dry edge because these values represent areas that are not covered by vegetation (Lu et al.

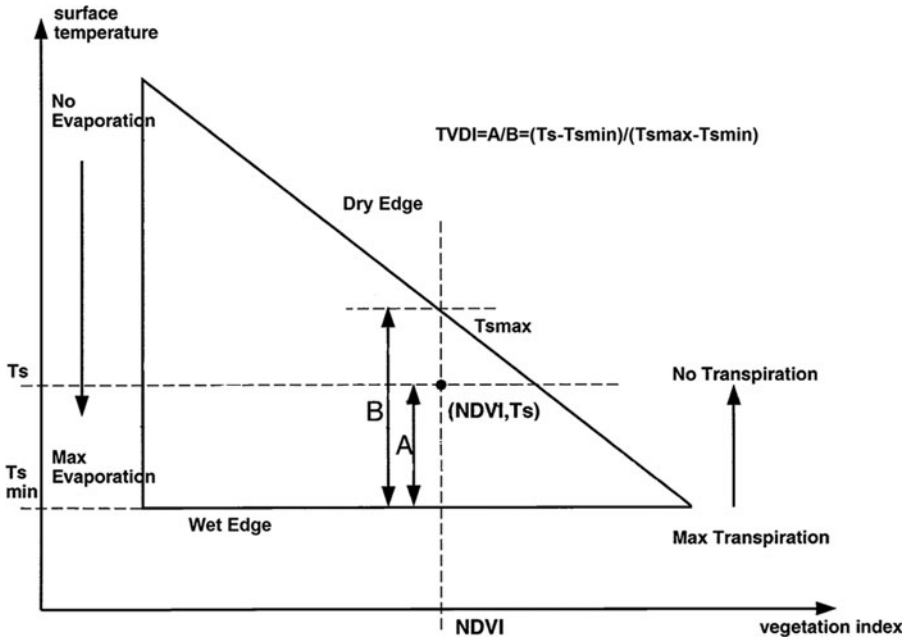

FIG. 4. Definition of the TVDI in a simplified triangular NDVI-Ts space (after Sandholt et al. 2002).

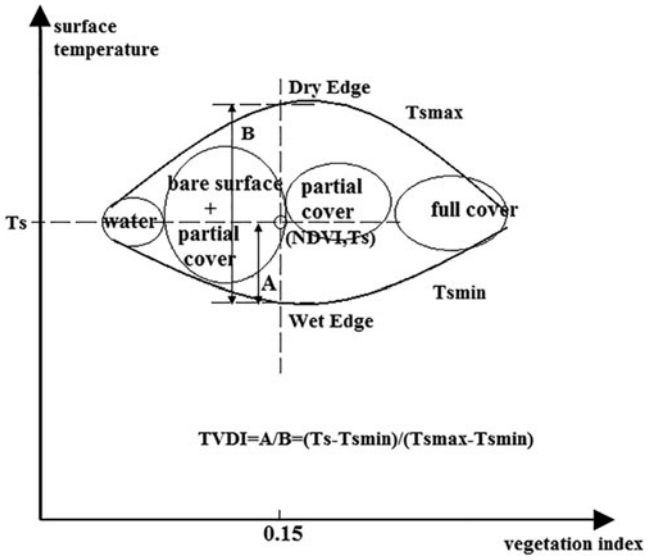

FIG. 5. Definition of TVDI in the biparabolic NDVI-T_s space.

2007). However, in this study, we found that the NDVI-T_s space is biparabolic, without a negative linear relationship between the NDVI and T_s, in arid and semiarid areas; most values of NDVI below 0.15 represent areas that are vegetated but have low biomass due to the arid conditions. However, when values of NDVI < 0.15 are omitted from the biparabolic NDVI-T_s space, the NDVI-T_s space becomes triangular (Figure 3b).

This study establishes a biparabolic NDVI-T_s space that includes the segment of the NDVI below 0.15 (Figure 5). The main land cover types in the biparabolic NDVI-T_s space are water, bare surface with partial cover, partial cover, and full cover. The principle of the biparabolic NDVI-T_s space is that the surface temperature of sunlit bare surface with partial cover is higher than that of sunlit water. The result is a rising trend in the dry edge when the NDVI < 0.15. Moreover, the NDVI can be expected to be negatively correlated with changes in T_s when NDVI > 0.15. The dry edge of the NDVI-T_s has been found to be useful in estimating land surface soil moisture and fractional vegetation cover (Han et al. 2006).

The fitting equations for the dry and wet edges in biparabolic NDVI-T_s space are as follows:

$$\begin{aligned} T_{s\,max} &= a_1 \times NDVI^2 + b_1 \times NDVI + c_1 \\ T_{s\,min} &= a_2 \times NDVI^2 + b_2 \times NDVI + c_2, \end{aligned} \quad [3]$$

where a_1, b_1, c_1, a_2, b_2, and c_2 are the fitting coefficients of the dry and wet edges that can be obtained from the scatter plot of the NDVI-T_s space. We note that Equation 3 has been developed for this dataset and application; it might require modification for use elsewhere.

VERIFICATION AND DISCUSSION

Scatter Plot of NDVI-T_s Space in the Validation Area

The Henan site was chosen as the validation area. Figure 6 shows that the NDVI-T_s space is a biparabola in Henan Province; the dry-edge position relationship has a high correlation coefficient $R^2 > 0.74$, and the wet-edge position relationship has a correlation coefficient $R^2 > 0.42$. The wet edge in the NDVI-T_s space changed from a parabola to approximately horizontal lines with increasing temperature and vegetation index.

Temporal and Spatial Evolution of Soil Moisture

Using the biparabolic NDVI-T_s space, Equation (1) was used to calculate the TVDI of the pixels with the dry and wet edges obtained from Equation (3). Soil moisture was classified into 5 categories: (*i*) very wet ($0 < \text{TVDI} \leq 0.2$); (*ii*) wet ($0.2 < \text{TVDI} \leq 0.4$); (*iii*) normal ($0.4 < \text{TVDI} \leq 0.6$); (*iv*) dry ($0.6 < \text{TVDI} \leq 0.8$); and (*v*) very dry ($0.8 < \text{TVDI} \leq 1$). Figures 7 and 8 show the spatial distribution of TVDI for the Shendong mining area and for Henan Province, respectively. The areas of Hongjiannao Lake in Figure 7 had the lowest TVDI.

Shendong Mining Area

Figure 7 shows that soil moisture conditions from TVDI with 500-m resolution are consistent with landform types in mining area.

(i) The western and southwestern portions of the mining area include a desert beach, which corresponds to region III (arid region) in Figure 7. These areas are covered in aeolian sandy soil, have weak soil capillary ability and low water-holding capacity, and are vulnerable to water and wind erosion.
(ii) Mobile sands, semifixed sand desertification of grassland, and steppe distribution are found in the southeastern and northwestern portions of the mining area and correspond with region II (normal area) in Figure 7.
(iii) Vegetation coverage in the eastern and northeastern portions of the mining area is high, corresponding to region I (humid area) in Figure 7. The type of soil in this region is loess, and its soil capillary ability and water-holding capacity are greater than those of sandy soil.

The results of using the biparabolic NDVI-T_s space to calculate the TVDI and to monitor soil moisture conditions in mining areas were essentially consistent with the landform types of the mining area and were reliable and credible.

Henan Province

Real-time daily precipitation data were used to validate the soil moisture distribution in Henan Province. The dynamic characteristics of soil moisture in Henan Province were as follows:

(i) From February 26, 2011 to March 13, 2011, soil moisture was low in the western, northeastern, and southern parts of

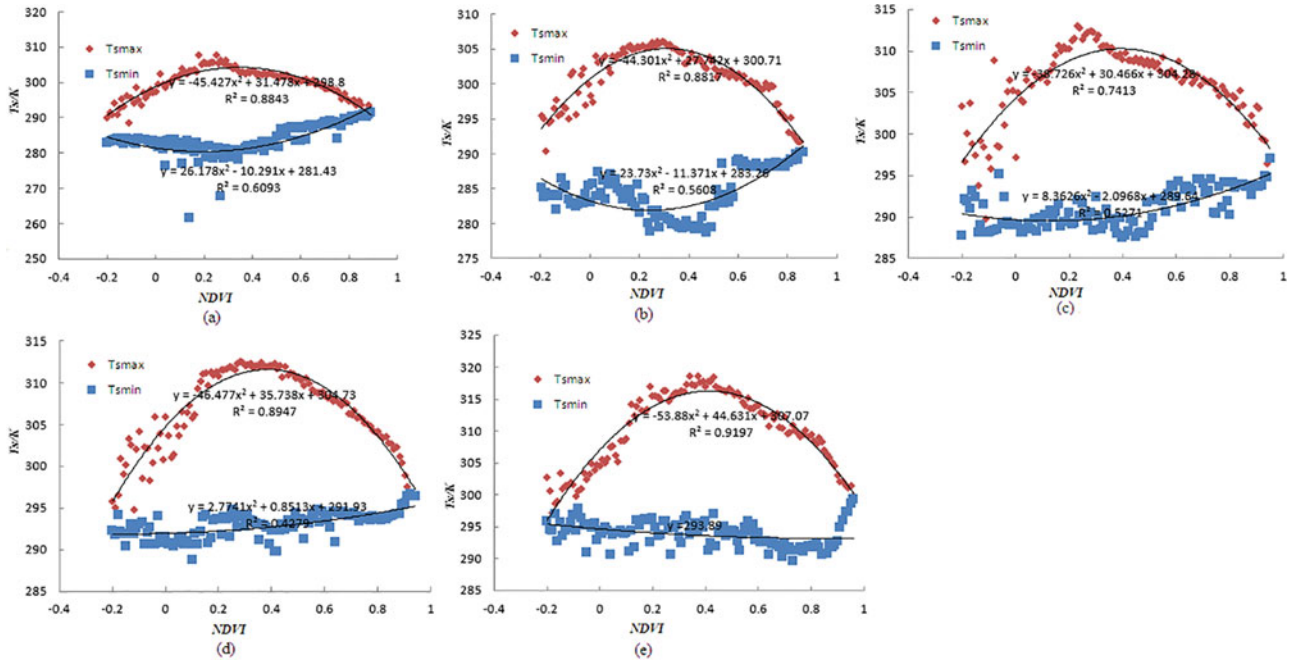

FIG. 6. Scatter plots of dry and wet edges in the NDVI-T_s space of Henan Province from February 26, 2011 to May 16, 2011: (a) 2/26/2011–3/13/2011; (b) 3/14/2011–3/29/2011; (c) 3/30/2011–4/14/2011; (d) 4/15/2011–4/30/2011; (e) 5/1/2011–5/16/2011.

Henan Province. On February 27, 2011 and March 1, 2011, precipitation covered the whole province, with maximum precipitation values of 16.88 mm and 14.9 mm, respectively, located mainly in the east. The minimum precipitation values were 1.69 mm and 1.02 mm, respectively, mainly located in the western part of Henan Province. Therefore, soil water content in the western part of Henan was low.

(ii) From March 14, 2011 to March 29, 2011, drought conditions were aggravated in the western and northeastern parts of Henan Province. Although precipitation occurred from March 20, 2011 to March 21, 2011, the precipitation values were only 4.36 mm and 9.77 mm, respectively, and the rainfall was quickly evaporated and absorbed. Hence, precipitation failed to relieve the drought conditions.

(iii) From March 30, 2011 to April 14, 2011, drought conditions were concentrated in the western part, but were relieved in the eastern part of the province. Precipitation occurred on April 3, 2011 and covered almost the whole province. The maximum precipitation was concentrated in the eastern area, which failed to alleviate the drought in the western part of Henan.

(iv) From April 15, 2011 to April 30, 2011, the drought eased in the west, but was aggravated in the southern part of Henan.

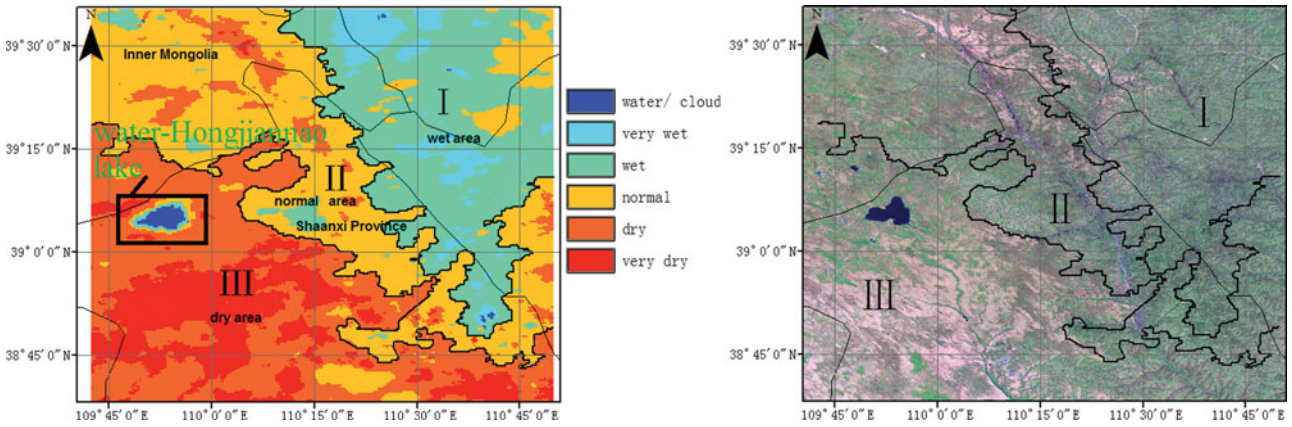

FIG. 7. Soil moisture grade distributions in the Shendong mining area.

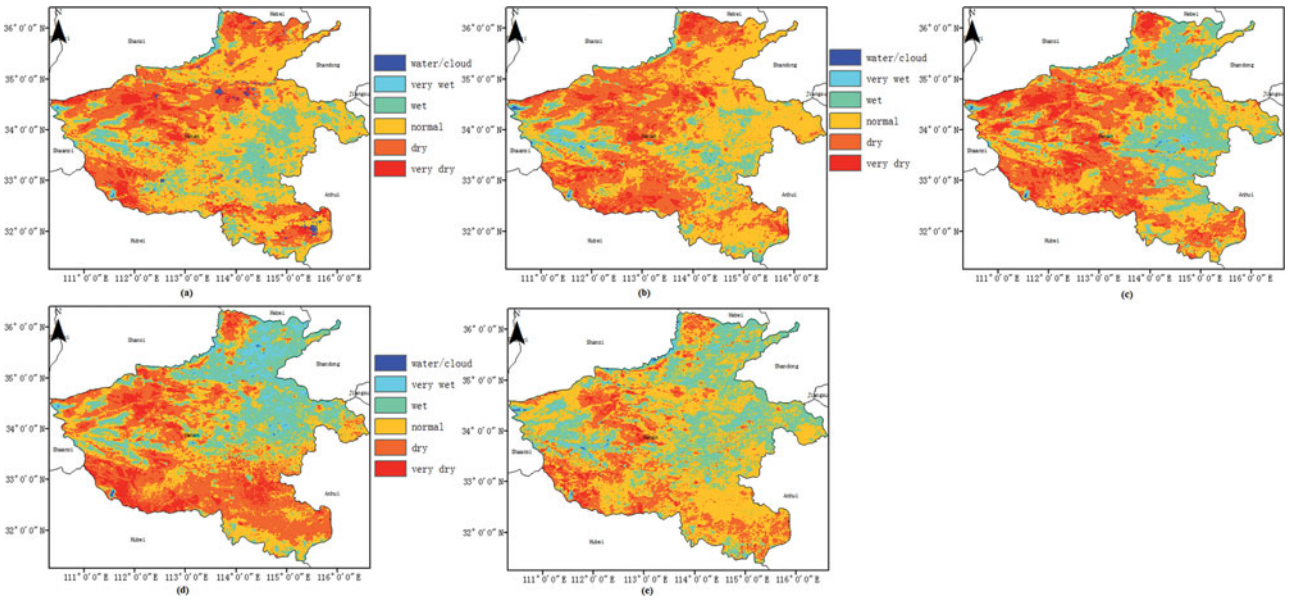

FIG. 8. Soil moisture grade spatiotemporal variation in Henan Province from February 26, 2011 to May 16, 2011: (a) 2/26/2011–3/13/2011; (b) 3/14/2011–3/29/2011; (c) 3/30/2011–4/14/2011; (d) 4/15/2011–4/30/2011; (e) 5/1/2011–5/16/2011.

TABLE 1
Linear correlation (R^2) between TVDI and 10-cm soil moisture in Henan Province

Time	$TVDI_C$	$TVDI_T$
26/2/2011–13/3/2011	0.3720***	0.2984**
14/3/2011–29/3/2011	0.2872**	0.2429*
30/3/2011–14/4/2011	0.3141**	0.1298
15/4/2011–30/4/2011	0.2931**	0.2771**
1/5/2011–16/5/2011	0.5270***	0.6183***

Note: ***,**,* represent significance levels of the coefficient of determination for $p < 0.01$, $p < 0.05$, and $p < 0.1$, respectively.

In addition to the southern region of Henan Province, precipitation occurred on April 21, 2011, which covered the whole province, with the maximum precipitation concentrated in the northeast.

(v) From May 1, 2011 to May 16, 2011, drought conditions were generally eased in the province. Precipitation covered the whole province on May 3, 10, and 11, 2011, which helped ease the drought conditions, effectively meeting the water needs of winter wheat in the filling stage.

TABLE 2
Linear correlation (R^2) between TVDI and 10-cm soil moisture in the Shendong mining area

	$TVDI_C$	$TVDI_T$
SM/%	0.3215***	0.0888

Note: *** represent significance levels of the coefficient of determination for $p < 0.01$.

Comparison of TVDI and Field-Measured Soil Moisture

Comparisons between TVDI and 10-cm-depth relative soil moisture data (SM) collected from the meteorological station of Henan Province and between TDVI and in-situ measurements of 10-cm-depth relative soil moisture data in the Shendong mining area were conducted. Taking SM as the abscissa and $TVDI_C$ obtained from the NDVI-T_s biparabolic spaces of Henan Province and the Shendong mining area, respectively, as ordinates, SM-

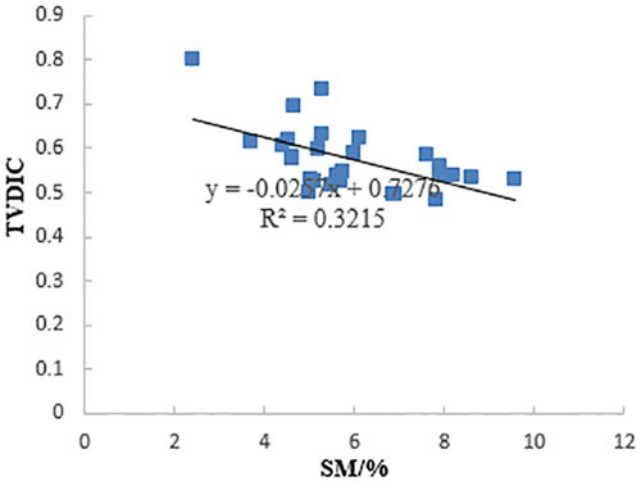

FIG. 9. Relationship between soil moisture at 10-cm depth and TVDI in the Shendong mining area.

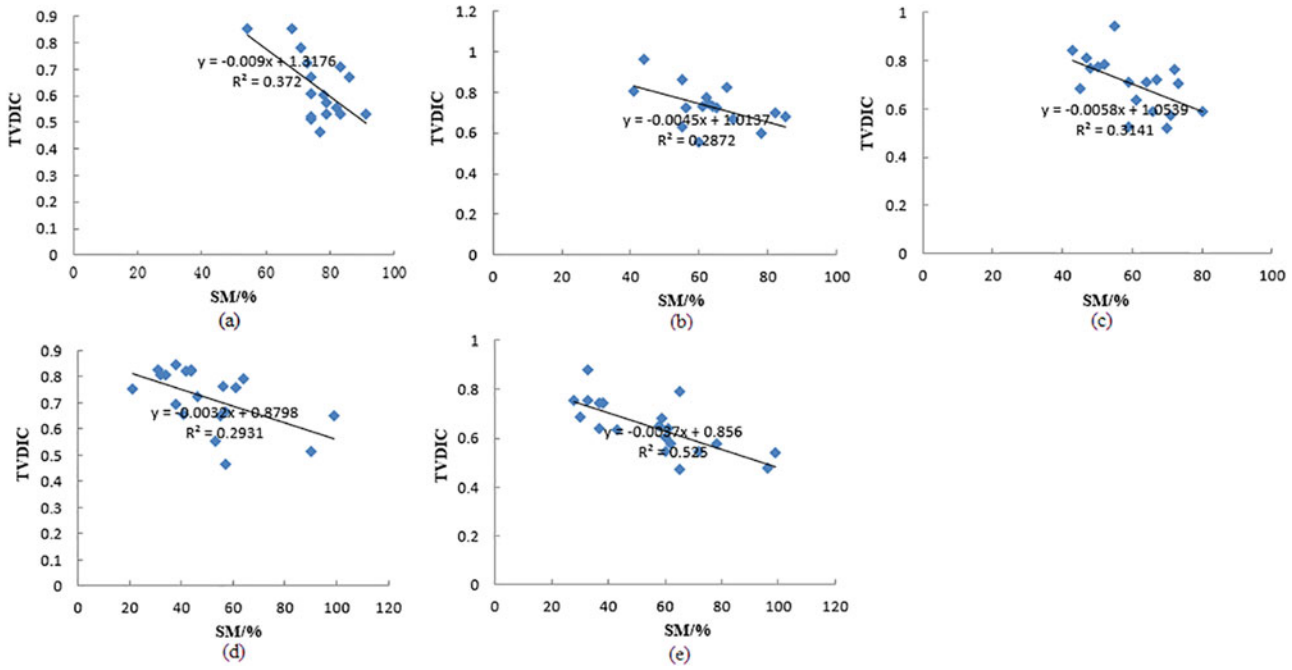

FIG. 10. Relationship between soil moisture at 10-cm depth and TVDI in Henan Province from February 26, 2011 to May 16, 2011: (a) 2/26/2011–3/13/2011; (b) 3/14/2011–3/29/2011; (c) 3/30/2011–4/14/2011; (d) 4/15/2011–4/30/2011; (e) 5/1/2011–5/16/2011.

TVDI scatter plots (Figures 9 and 10) were constructed and then compared with the $TVDI_T$ obtained from the triangular NDVI-T_s space. Correlation coefficients were also calculated (Tables 1 and 2).

Figures 9 and 10 and Tables 1 and 2 show that higher soil moisture values correspond to lower TVDI values. Linear relationships exist between TVDI and relative soil moisture, with $R^2 > 0.28$. The F-test found that the regression equation relating 10-cm-depth SM to different periods of $TVDI_C$ in Henan Province and the Shendong mining area passed the significance test ($p = 0.05$). The results showed that the biparabolic NDVI-T_s space is slightly better than the triangular NDVI-T_s space for monitoring soil moisture conditions and that $TVDI_C$ is better than $TVDI_T$ for assessing 10-cm-depth soil moisture conditions.

The correlation coefficient between soil moisture and TVDI was not very high (Figures 9 and 10) because 1-km and 500-m resolution MODIS data are difficult to correlate precisely with weather-station and field-measured soil moisture values. However, meteorological weather-station data can represent the average meteorological characteristics in a region. Therefore, weather-station data and field-measured soil moisture can be used to validate TVDI.

The land cover in the area with NDVI < 0.15 is almost totally grassland, with low biomass at the Shendong site. In Henan Province, the main land use types in the portions with NDVI < 0.15 are buildings and farmland. Farmland other than water and buildings makes up about 22.39% of the total area with NDVI < 0.15.

When TVDI was calculated from the biparabolic and triangular NDVI-T_s spaces, the results obtained from the 2 kinds of space were similar. However, when comparing TVDI with field-measured soil moisture data, the correlation between 10-cm-depth soil moisture and TVDI obtained from the biparabolic NDVI-T_s space was slightly better than with TDVI obtained from the triangular space. Therefore, the area with NDVI $<$ 0.15 should be included in the biparabolic NDVI-T_s space and should not be omitted, and water bodies can also be recognized by the biparabolic NDVI-T_s space.

CONCLUSIONS

Unlike linear dry and wet edges in triangular NDVI-T_s space, dry and wet edges in this research exhibited a parabolic shape in a scatter plot of T_s and NDVI. Taking the Shendong mining area as the experimental site and Henan Province as the validation site, the NDVI-T_s space was found to be biparabolic in arid and semiarid areas where most areas with NDVI below 0.15 are vegetated but have low biomass due to the arid conditions. TVDI derived from biparabolic NDVI-T_s and TVDI obtained from triangular NDVI-T_s space were compared with relative soil moisture. It was shown that TVDI derived from biparabolic NDVI-T_s was slightly better than that derived from triangular NDVI-T_s space. The biparabolic NDVI-T_s space complements the triangular NDVI-T_s space in that TVDI derived from biparabolic NDVI-T_s space can estimate accurately the soil moisture conditions at 10-cm depth.

ACKNOWLEDGMENTS

We owe special thanks to Baodong Ma and two anonymous reviewers for thorough and excellent reviews of earlier versions of this manuscript.

FUNDING

This work was jointly supported by the National Basic Research Program of China (973 Program) (Grant No. 2011CB707102) of the China Ministry of Science, the National Natural Science Foundation of China (Grant No. 41401496), Scientific research program of Shaanxi Educational Committee (Grant No. 14JK1471), Doctoral scientific research foundation (Grant No. 2014QDJ060) and Research Development Fund (Grant No.201305) of Xi'an University of Science and Technology.

REFERENCES

Carlson, T.N., Gillies, R.R., and Perry, E.M. 1994. "A method to make use of thermal infrared temperature and NDVI measurements to infer surface soil water content and fractional vegetation cover." *Remote Sensing Reviews*, Vol. 9(No. 1–2): pp. 161–173.

Carlson, T. 2007. "An overview of the 'triangle method' for estimating surface evapotranspiration and soil moisture from satellite imagery." *Sensors*, Vol. 7(No. 8): pp. 1612–1629.

Chen J., Wang, C.Z., Hong, H., Liu, X.M., and Zhen, R.Y. 2011. "Estimating soil moisture using temperature-vegetation dryness index (TVDI) in the Huang-huai-hai (HHH) plain." *International Journal of Remote Sensing*, Vol. 32(No. 4): pp. 1165–1177.

Gao Z.Q., Gao, W., and Chang, N.B. 2011. "Integrating temperature vegetation dryness index (TVDI) and regional water stress index (RWSI) for drought assessment with the aid of LANDSAT TM/ETM +images." *International Journal of Applied Earth Observation and Geoinformation*, Vol. 13(No. 3): pp. 495–503.

Gillies, R.R., and Carlson, T.N. 1995. "Thermal remote sensing of surface soil water content with partial vegetation cover for incorporation into climate models." *Journal of Applied Meteorology*, Vol. 34 (No. 4): pp. 745–756.

Girolimetto, D., and Venturini, V. 2013. "Water stress estimation from NDVI-T_s plot and the wet environment evapotranspiration." *Advanced Remote Sensing*, Vol. 2: pp. 283–291.

Goward, S.N., Cruickhanks, G.D., and Hope, A.S. 1985. "Observed relation between thermal emission and reflected spectral radiance of a complex vegetated landscape." *Remote Sensing of Environment*, Vol. 18(No. 2): pp. 137–146.

Goward, S.N., and Hope, A. S. 1989. "Evapotranspiration from combined reflected solar and emitted terrestrial radiation: Preliminary FIFE results from AVHRR data." *Advances in Space Research*, Vol. 9(No. 7): pp. 239–249.

Han, L.J., Wang, P.X., Yang, H., Liu, S.M., and Wang, J.D. 2006. "Study on NDVI-T_s space by combining LAI and evapotranspiration." *Science in China (D Series): Earth Sciences*, Vol. 49(No. 7): pp. 747–754.

Han, Y., Wang, Y.Q., and Zhao, Y.S. 2010. "Estimating soil moisture conditions of the Greater Changbai Mountains by land surface temperature and NDVI." *IEEE Tractions on Geoscience and Remote Sensing*, Vol. 48(No. 6): pp. 2509–2515.

Hope, A.S., Petzold, D.E., Goward, S.N., and Robert, M. R. 1986. "Simulated relationship between spectral reflectance, thermal emissions and evapotranspiration of a soybean canopy." *Journal of the American Water Resources Association*, Vol. 22(No. 6):pp. 1011–1019.

Juliena, Y., Sobrinoa, J.A., Mattar, C., Ruescas, A.B., Jiménez-Muñoza, J.C., Sòria, G., Hidalgoa, V., Atitara, M., Francha, B., and Cuenca, J. 2011. "Temporal analysis of normalized difference vegetation index (NDVI) and land surface temperature (LST) parameters to detect changes in the Iberian land cover between 1981 and 2001." *International Journal of Remote Sensing*, Vol. 32(No. 7): pp. 2057–2068.

Karnieli, A., Agam, N., Pinker, R.T., Anderson, M., Imhoff, M.L., Gutman, G.G., Panov, N., and Goldberg, A. 2010. "Use of NDVI and land surface temperature for drought assessment: merits and limitations." *Journal of Climate*, Vol. 22(No. 3):pp. 618–633.

Lambin, E.F., and Ehrlich, D. 1996. "The surface temperature-vegetation index space for land cover and land-cover change analysis." *International Journal of Remote Sensing*, Vol. 17 (No. 3): pp. 463–487.

Li, X. B., Wang, H., Long, H.L., Wei, D.D., and Bao, Y. 2012. "A model for the estimation of fractional vegetation cover based on the relationship between vegetation and soil moisture." *International Journal of Remote Sensing*, Vol. 33(No. 11): pp. 3580–3595.

Lu, Y., Tao, H.P., and Wu, H. 2007. "Dynamic drought monitoring in Guangxi using revised temperature vegetation dryness index." *Wuhan University Journal of Natural Sciences*, Vol. 12(No. 4): pp. 663–668.

Moran, M., Clarke, T., Inoue, Y., and Vidal, A. 1994. "Estimating crop water deficit using the relation between surface-air temperature and spectral vegetation index." *Remote Sensing of Environment*, Vol. 49(No. 3): pp. 246–263.

Muñoz-Sabater, J. 2015. "Incorporation of passive microwave brightness temperatures in the ECMWF soil moisture analysis." *Remote Sensing*, Vol. 7(No. 5): pp. 5758–5784.

Nemani, R.R., and Running, S.W. 1989. "Estimation of regional surface resistance to evapotranspiration from NDVI and thermal IR AVHRR data." *Journal of Applied Meteorology*, Vol. 28(No. 4): pp. 276–284.

Nemani, R.R., Pierce, L., Running, S.W., and Goward, S.N. 1993. "Developing satellite-derived estimates of surface moisture status." *Journal of Applied Meteorology*, Vol. 32(No. 3): pp. 548–557.

Price, J.C. 1990. "Using spatial context in satellite data to infer regional scale evapotranspiration." *IEEE Tractions on Geoscience and Remote Sensing*, Vol. 28(No. 5): pp. 940–948.

Rahimzadeh-Bajgiran, P., Omasa, K., and Shimizu, Y. 2012. "Comparative evaluation of the Vegetation Dryness Index (VDI), the Temperature Vegetation Dryness Index (TVDI) and the improved TVDI (iTVDI) for water stress detection in semi-arid regions of Iran." *ISPRS Journal of Photogrammetry and Remote Sensing*, Vol. 68: pp. 1–12.

Sandholta, I., Rasmussena, K., and Andersen, J. 2002. "A simple interpretation of the surface temperature/ vegetation index space for assessment of surface moisture status." *Remote Sensing of Environment*, Vol. 79(No. 2–3): pp. 213–224.

Sela, S., Svoray, T., and Assouline, S. 2012. "Soil surface sealing effect on soil moisture at a semiarid hillslope: implications for remote sensing estimation." *Remote Sensing*, Vol. 6(No. 8): pp. 7469–7490.

Skierucha, W., Wilczek, A., Szypłowska, A., Sławiński, C., and Lamorski, K. 2014. "A TDR-based soil moisture monitoring system with

simultaneous measurement of soil temperature and electrical conductivity." *Sensors*, Vol. 12(No. 10): pp. 13545–13566.

Sona, N.T., Chen, C.F., Chen, C.R., Changa, L.Y., and Minhc, V.Q. 2012. "Monitoring agricultural drought in the Lower Mekong Basin using MODIS NDVI and land surface temperature data." *International Journal of Applied Earth Observation and Geoinformation*, Vol. 18: pp. 417–427.

Sun, L, Sun, R., Li, X.W., Liang, S.L., and Zhang, R.H. 2012. "Monitoring surface soil moisture status based on remotely sensed surface temperature and vegetation index information." *Agricultural and Forest Meteorology*, Vol. 166, 175–187.

Sun, Z.G., Wang, Q.X., Matsushita, B.K., Fukushima, T., Zhu, O.Y., and Zhen, R.Y. 2011. "Evaluation of the VI-T_s method for estimating the land surface moisture index and air temperature using ASTER and MODIS data in the North China Plain." *International Journal of Remote Sensing*, Vol. 32(No. 22): pp. 7257–7278.

Tang, R.L., Li, Z.L., and Tang, B.H. 2010. "An application of the T_s-VI triangle method with enhanced edges determination for evapotranspiration estimation from MODIS data in arid and semi-arid regions: Implementation and validation." *Remote Sensing of Environment*, Vol. 114(No. 3): pp. 540–551.

Wang, P.X., Li, X.W., Gong, J.Y., and Song, C.H. 2001. "Vegetation temperature condition index and its application for drought monitoring." Paper presented in Proceedings of International Geoscience and Remote Sensing Symposium, Sydney, Australia, July 9–13, 2001.